A Phosphorescent Soft Salt Based on Platinum(II) Complexes: Photophysics, Self-Assembly, Thermochromism, and Anti-Counterfeiting Application

Yun Ma[1,2], Kexin Chen[1], Jinyu Lu[1], Jiandong Shen[1], Chenxi Ma[1], Shujuan Liu[1], Qiang Zhao[1,], Wai-Yeung Wong[2,3,]**

[1] State Key Laboratory of Organic Electronics and Information Displays and Institute of Advanced Materials (IAM), Nanjing University of Posts and Telecommunications (NUPT), 9 Wenyuan Road, Nanjing 210023, Jiangsu, P. R. China

[2] Department of Applied Biology and Chemical Technology, The Hong Kong Polytechnic University, Hung Hom, Hong Kong, P. R. China

[3] Hong Kong Polytechnic University Shenzhen Research Institute, Shenzhen 518057, P. R. China

KEYWORDS: phosphorescent soft salts, stimuli-responsive materials, metal-metal interactions, time-resolved imaging, anti-counterfeiting application

ABSTRACT

A new platinum(II) complex based soft salt **S1**, ($[Pt(tpp)(ed)]^{+}[Pt(pba)(CN)_2]^{-}$) (tpp = 2-(4-(trifluoromethyl)phenyl)pyridine, ed = ethane-1,2-diamine, pba = 4-(2-pyridyl)benzaldehyde), was designed and synthesized. UV-visible absorption and photoluminescence (PL) spectra were studied to elucidate the nature of ground and excited states. The soft salt complex was found to show self-assembly properties with the assistance of electrostatic, π–π stacking, and Pt···Pt interactions, resulting in the remarkable emergence of low-energy absorption and PL bands. Morphological transformation of **S1** from undefined nano-sized aggregates to nanofibers under different solvent compositions has been demonstrated. Interestingly, a luminescent polymer film was prepared by doping **S1** into a polyethylene glycol (PEG) matrix. The film displayed distinctive emission color change from yellow to red upon heating. Eventually, a high-level anti-counterfeiting application was accomplished by time-resolved imaging technique based on the thermochromic luminescence property and long emission decay time displayed by **S1**. It is anticipated that this work can provide deep insights into the control of intermolecular interactions between cationic and anionic complexes of soft salt upon exposure to different external stimuli, resulting in the development of smart luminescent materials for various applications.

1. INTRODUCTION

Stimuli-responsive luminescent materials have been of topical research interest in recent years due to their growing demand in various optoelectronic applications, such as in memory devices,[1] molecular switches,[2] optical imaging,[3] information encryption and decryption,[4] anti-counterfeiting,[5] and so on. In this context, a significant number of photochromic,[6] electrochromic,[7] mechanochromic,[8] vapochromic,[9] and thermochromic[10] materials have been developed based on

small molecules,[11] metal complexes,[12] polymers,[13] and nanomaterials.[14] Among these, phosphorescent transition-metal complexes, which display high photoluminescence (PL) quantum yields, remarkable photostability, tunable luminescence colors, and increased sensitivity to external stimuli, are promising for designing excellent smart luminescent materials.[15]

Recently, a newly emerging class of ion-paired complexes of soft salts formed by two oppositely charged luminescent transition-metal complexes have aroused considerable attention because of their interesting structural and intriguing photophysical properties.[16] The easily tunable PL properties of these soft salt complexes have accelerated the studies on their potential in diverse optoelectronic applications, including organic light-emitting diodes,[17] bioimaging,[18] photodynamic therapy,[19] etc. Considering the fact that distinct emission wavelengths can be easily obtained in a soft salt by molecular engineering of the ligands of ionic complexes, it can serve as a perfect platform for designing smart luminescent materials. Besides, compared to fluorescent molecules, phosphorescent transition-metal complexes exhibit attractive long emission lifetimes in the range of hundred nanoseconds to a few microseconds,[20,21] which is advantageous to biological imaging and anti-counterfeiting areas.[22] This is because multilevel dimensions can be obtained when the emission lifetime is used as a signal to analyze the information by using photoluminescence lifetime imaging microscopy (PLIM). To date, however, the application of phosphorescent soft salts in this research area has barely been exploited.

Soft salts based on platinum(II) complexes are thought to be ideal candidates for the construction of stimuli-responsive luminescent systems, because: (i) these complexes have been reported to show fantastic optical properties on account of metal−metal and π−π stacking interactions,[23] and (ii) the electrostatic interactions between anionic and cationic components facilitate the formation of very close metal-metal interactions. Thus, the optical properties of these soft salt complexes can

be tailor-made to be responsive to various external stimuli by precisely regulating various intermolecular interactions. In keeping with these facts, a phosphorescent soft salt based on two platinum(II) complexes has been designed and synthesized in this work. The platinum(II) complex **C1** ($[Pt(tpp)(ed)]^+Cl^-$, tpp = 2-(4-(trifluoromethyl)phenyl)pyridine, ed = ethane-1,2-diamine) was selected as the cationic component, and the platinum(II) complex **A1** ($[Pt(pba)(CN)_2]^-Bu_4N^+$, pba = 4-(2-pyridyl)benzaldehyde) was chosen as the anionic component. The cationic and anionic components were combined to construct the soft salt complex **S1** ($[Pt(tpp)(ed)]^+[Pt(pba)(CN)_2]^-$) via Van der Waals force and electrostatic interactions (Figure 1). This new soft salt complex **S1** showed interesting changes in its optical properties upon varying the solvent composition. Such changes were demonstrated to be associated with the formation of well-defined nanostructures. Also, a thermochromic luminescent film was prepared by blending **S1** into a polyethylene glycol (PEG) matrix, and it was successfully employed to create high level security anti-counterfeiting labels by applying the time-resolved imaging technique.

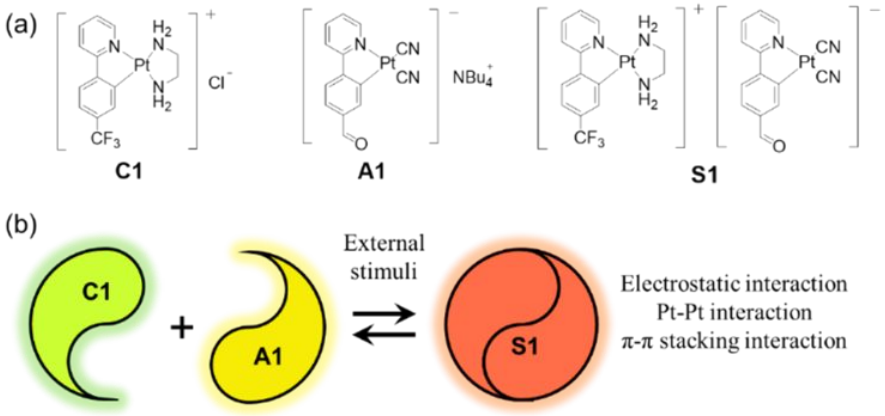

Figure 1. (a) Chemical structures of complexes **A1**, **C1** and **S1**. (b) Design concept of the construction of the stimuli-responsive material based on a soft salt.

2. RESURTS AND DISCUSSION

The cationic platinum(II) complex **C1** was synthesized by Stirring the platinum(II) dichloro-bridged dimer with ethylenediamine (3 equiv.) in dichloromethane, and the anionic platinum(II) complex **A1** was prepared by stirring platinum(II) dichloro-bridged dimer and tetrabutylammonium cyanide (5 equiv.) in dichloromethane at 50 °C for 6 h. The soft salt complex **S1** was obtained by mixing oppositely charged platinum(II) complexes **A1** and **C1** (1 : 1.1 molar ratio) in EtOH/H_2O (1 : 10, v / v) *via* metathesis reaction. The desired platinum(II) complexes were characterized by electrospray ionization mass spectrometry (ESI-MS) mass spectrometry, ^1H and ^{13}C nuclear magnetic resonance (NMR) spectroscopy. A titration experiment was conducted by mixing **C1** and **A1** in methanol solution. As shown in Figure S1, a binding stoichiometry of 1:1 was clearly obtained from the Jobs' plot, suggesting the 1:1 molar ratio of the two components.

Table 1. Photophysical properties of **A1**, **C1**, and **S1**

Complex	Medium (298 K)	Absorption λ_{max}/nm (ε/dm^3 mol^{-1} cm^{-1})	Emission λ_{max}/nm (τ_o/μs)	Φ (%)
C1	MeOH	275 (16650), 308 (6620), 322 (5540), 342 (3570), 388 (1980)	491, 527 (0.6)	1.03
	DMSO	277 (20850), 308 (8820), 320 (7560), 346 (4860), 390 (2690)	483, 518, 562 (5.3)	
	Solid		500, 532 (2.3)	3.44
A1	MeOH	289 (20590), 320 (11010), 332 (11540), 390 (2740)	532, 566 (4.8)	0.13
	DMSO	292 (19880), 321 (12060), 334 (11850), 392 (2750)	522, 566 (5.3)	
	Solid		526, 570 (10.9)	23.63
S1	MeOH	275 (28460), 289 (23890), 320 (14400), 342 (13240), 385 (4032)	491, 527, 566 (4.8)	0.26
	DMSO	280 (49982), 298 (41182), 322 (29151), 335 (24607), 381 (7492)	491, 530, 567 (5.1)	
	Solid		692 (0.3)	6.17

The photophysical properties of the precursor ionic platinum(II) complexes **C1** and **A1**, and the soft salt complex **S1** have been studied. The UV/visible absorption spectra of **C1** and **A1** in DMSO exhibited very intense ligand centered (LC) transition at 280 and 292 nm (Figure 2a and Table 1).

The lower absorptions in the range from 300 to 350 nm are absent in the absorption spectra of the pba and tpp ligands (Figure S2), which is indicative of the metal-to-ligand charge transfer (MLCT) transition of these absorption bands. The low-energy absorption tails above 380 nm are assigned to the spin-forbidden ligand-centered (^{3}LC) transitions.[24]

The room temperature emission spectrum of **C1** and **A1** displayed sharp-structured emission bands in the range of 483 to 566 nm in DMSO solution (1×10^{-5} M). Generally, the structured emission profile at room temperature is indicative of ligand centered character.[25] In addition, the PL spectral profiles of the frozen CH_3OH solution of **C1** and **A1** at 77 K are almost unchanged compared to those at room temperature. Therefore, we can conclude that the ^{3}LC state participates in the emissions for **C1** and **A1** (Figures 2c and 2d). Complex **S1** showed the mixed emission band of **C1** and **A1** in the solution, and it also displayed similar emission profile at low temperature.

As presented in Figure 2a, DMSO solution of the soft salt complex **S1** (1×10^{-5} M) at room temperature displayed ^{1}LC, ^{3}LC, and MLCT transitions in the absorption spectrum. The absence of additional lower-energy absorption bands indicates that the complex **S1** exists as discrete charged species in DMSO solution even at a concentration of 1.5×10^{-3} M (Figure S3). Upon increasing the proportion of H_2O in DMSO solution, its color changes from colorless (pure DMSO) to red (DMSO : H_2O, v : v, 1 : 5), accompanied by an emergence of a new absorption band at around 514 nm with an obvious isosbestic point (Figure 2b). This new absorption peak is ascribed to metal−metal-to-ligand charge transfer (MMLCT) transitions, which originate from the Pt···Pt and/or π−π stacking interactions between the two oppositely charged platinum(II) complexes.[26] In addition, for the soft salt complex **S1**, with increasing the H_2O portion, the emergence of the MMLCT transition peaks in the UV−vis absorption spectrum was accompanied by the appearance of a new emission band at 680 nm when excited at 365 nm in DMSO (Figure 2e). This newly

emerged emission peak in the presence of high-water content is assigned to the ^{3}MMLCT emission, which originates from Pt···Pt and π–π stacking interactions between the cationic and anionic complexes.[27] However, a similar observation is absent for **C1** and **A1** complexes on changing the solvent compositions. Also, complexes **C1**, **A1** and **S1** showed distinct PL properties in the solid-state (Figure 2f). These photophysical data confirm that the electrostatic interaction between two oppositely charged species is responsible for the Pt···Pt and π–π stacking interactions.

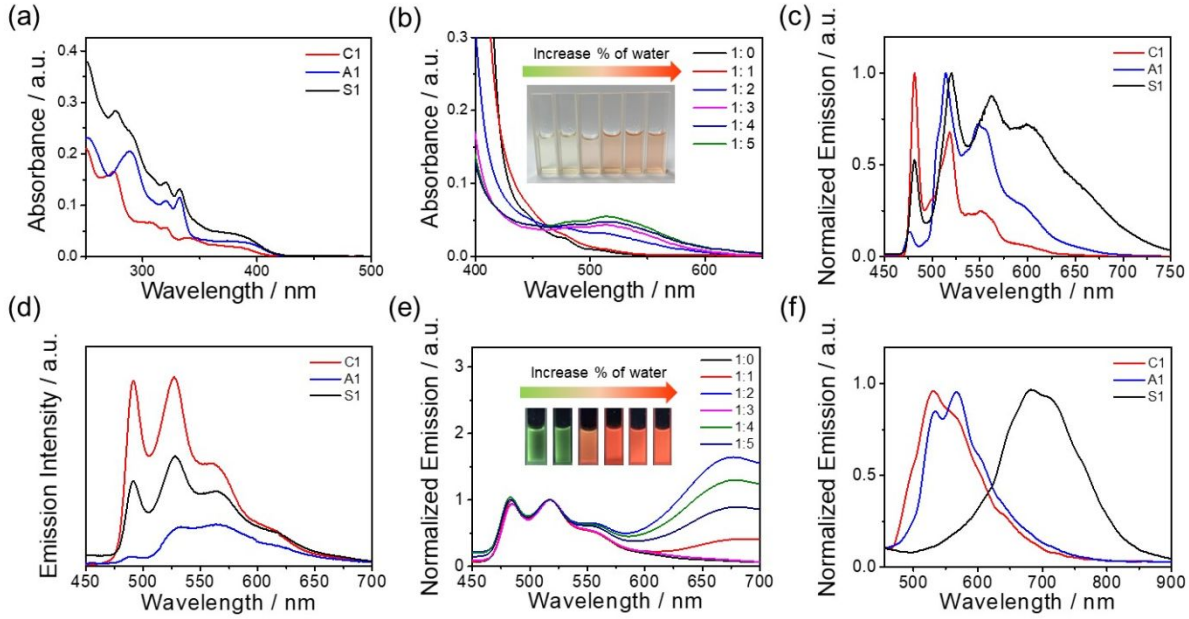

Figure 2. (a) UV−vis absorption spectra of **C1**, **A1**, and **S1** in DMSO solution. (b) UV−vis absorption spectra of **S1** in DMSO-H_2O mixture (1×10^{-3} M) with different H_2O fractions. The inset shows photos of **S1** (1×10^{-3} M) upon increasing the water content in DMSO. (c) PL spectra of **C1**, **A1**, and **S1** in CH_3OH solution at 77 K. (d) PL spectra of **C1**, **A1**, and **S1** in DMSO solution. (e) PL spectra of **S1** in DMSO-H_2O mixture (1×10^{-3} M) with different H_2O fractions. The inset shows PL photos of **S1** (1×10^{-3} M) upon increasing the water content in DMSO upon excitation at 365 nm. (f) PL spectra of **C1**, **A1**, and **S1** in the solid state.

^{1}H NMR spectra at different DMSO-water compositions were recorded to study the aggregation behavior of the two ionic components. The soft salt complex **S1** was found to show the aggregation in DMSO with increasing water content. As shown in Figure 3, well-resolved proton signals with clear splitting patterns corresponding to **S1** can be observed in DMSO-d_6. Increasing the D_2O content resulted in poorly resolved and broad proton signals which reached complete obscurity at D_2O content of 40%. This result is consistent with the findings obtained in the previous reports,[23] indicating the presence of a substantial extent of π−π stacking interactions between the two oppositely charged ions at high water contents.

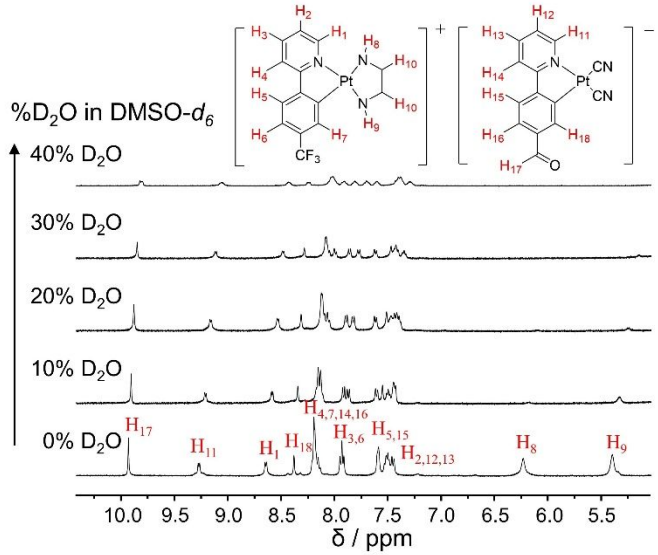

Figure 3. ^{1}H NMR spectral changes at different contents of D_2O in DMSO-d_6 for **S1** (5×10^{-3} M).

A transmission electron microscope (TEM) was used to identify the morphology of the soft salt complex **S1** in DMSO solution and DMSO/H_2O mixture (DMSO : H_2O, v : v, 1 : 3), and to explain the UV−vis absorption and PL spectral changes, as well as the NMR experiments. As shown in Figure S5, the TEM image indicates the lack of well-defined nano-sized aggregates in DMSO solution (1.5×10^{-3} M), which is in accordance with the photophysical data obtained in DMSO. In addition, the self-assembly properties of **A1** and **C1** in the same solvent compositions have been

studied. Figure S6 showed the lack of well-defined nano-sized aggregates of **A1** and **C1** (1.5×10^{-3} M) in such conditions. Conversely, TEM image of **S1** prepared from DMSO/H_2O mixture under the same concentration results in the formation of uniform nanofibers with a width of around 50 nm and lengths ranging from 1 to 3 μm (Figures 4a). Selected area electron diffraction (SAED) analysis was employed to determine the molecular packing of the nanofibers. As shown in Figure 4b, the obvious diffraction confirms its crystalline nature. It is worth noting that one d spacing is about 0.346 nm (Figure S7), which is indicative of the presence of periodic Pt···Pt and π-π interactions in the self-assembled nanostructure. Therefore, as presented in Figure 4c, a process for the assembly of **S1** to form nanofiber is suggested. **S1** dissolves very well in pure DMSO without any noticeable aggregation between the cations and anions. Nevertheless, with the increased portion of water in DMSO, oppositely charged cations and anions would come into close proximity to form ion pairs to avoid the unfavorable contacts with the water molecules. Finally, the alternate stacking of cations and anions would give rise to the assembly of one-dimensional nanofiber with the assistance of electrostatic, Pt···Pt and π−π stacking interactions. The formation of nanofiber would also result in the poorly resolved and broad proton signals as well as the ^{3}MMLCT absorption and PL bands.

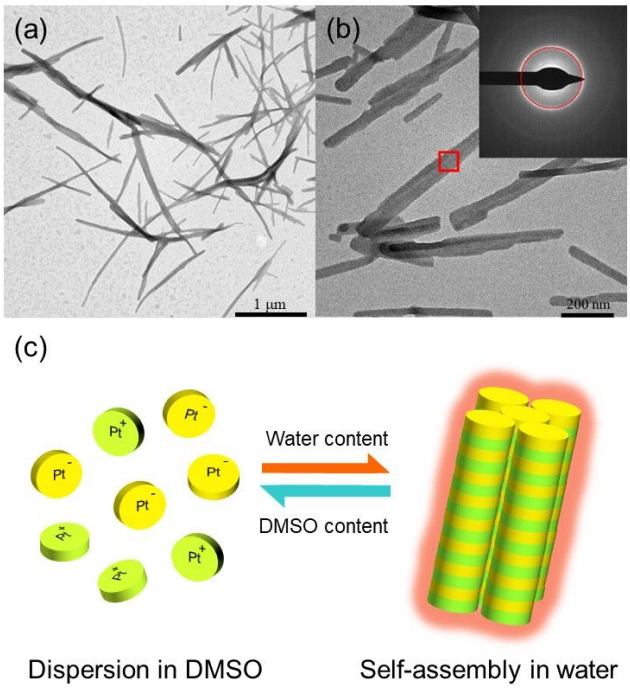

Figure 4. (a) and (b) TEM images of the nanostructure obtained from **S1** (1.5×10^{-3} M) in DMSO/H_2O mixture (DMSO : H_2O, v : v, 1 : 3). (c) Schematic illustration of the self-assembled **S1** to form the nanofiber.

Having gained a deep insight into the modulation of the photophysical properties of the soft salt complex **S1** by various non-covalent intermolecular interactions between two oppositely charged ions, the development of **S1** into a stimuli-responsive luminescent material was further explored. A thermochromic luminescent material (TLM) was designed and prepared by incorporating the soft salt complex **S1** into a well-known thermoplastic polymer polyethylene glycol (PEG). Typically, internal micro-environments of PEG matrix would be altered upon heating due to the increase in free volume and polymer chain movement.[28] This variation was sufficient to alter the intermolecular interactions between the two oppositely charged ions and consequently result in luminescence color changes. To test this hypothesis, the PL spectral changes of PEG8000 film with different concentrations of **S1** were studied as the first step. As displayed in Figures 5a and 5b, when the **S1** content was increased from 0.1 to 5.0 wt %, green and yellow emissions were

obtained. The PL spectrum of **S1** was dependent on its concentration in the PEG film. The intensity ratio of emission bands of luminescent ions and ^{3}MMLCT peaks changed remarkably depending on the **S1** concentration. Upon excitation at 365 nm, at a low concentration of 0.1 wt%, the emission was observed primarily from the cationic and anionic components. This is because the polymeric chains tended to separate out of two ions at low concentration. With the increase in concentration of the soft salt complex in PEG matrix, a new emission peak from the ^{3}MMLCT transition appeared as a result of the coming together of the cations and anions.

Next, the PEG8000 films (m.p. ≈ 62 °C) prepared with different concentrations of **S1** (from 0.1 wt% to 5 wt%) were heated to 60 °C. As shown in Figures 5c and S3, the PL spectra and emission colors hardly showed any change below the concentration of 3 wt%, while the PL spectra displayed a significant enhancement at 680 nm for the ones containing **S1** at 3-5 wt% concentrations. For example, when 5 wt% of **S1** was blended into PEG8000, the resulting polymer film showed a yellow emission upon UV excitation at 365 nm. As illustrated in Figures 6c and 6d, the intensity of ^{3}MMLCT band at 680 nm increased continuously while the intensity of the yellow emission peak at around 568 nm decreased as the temperature rose to 60 °C. After the temperature recovered back to room temperature, the emission color once again changed from red to yellow. As shown in Figure 6f, the temperature-dependent PL spectral changes of **S1**/PEG8000 film were repeated 10 cycles at both 25 and 60 °C with no detectable intensity variations, suggesting the excellent reversibility of the system.

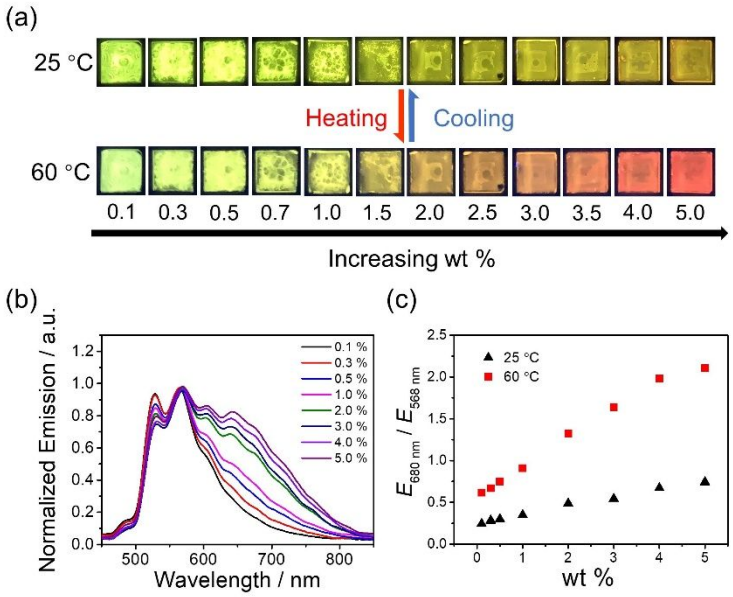

Figure 5. (a) PL photographs of **S1** in PEG8000 films at different concentrations (0.1 wt% to 5.0 %) upon heating to 60 °C (excitation at 365 nm). (b) PL spectra of **S1** in PEG8000 films at different concentrations (0.1 wt% to 5.0 %). (c) The comparison of emission variations between 25 °C and 60 °C in different **S1**/PEG8000 films.

In addition, the relative sensitivity of **S1**/PEG8000 was measured by using the equation Sr = $(\partial(E_{680}/E_{568})/\partial T)/(E_{680}/E_{568})$, where E_{680}/E_{568} is the intensity ratio of the two emission bands.[29] In the range of 25 to 60 °C, the calculated sensitivity of **S1**/PEG8000 was high with its maximum value reaching 2.78% per degree (Figure 6e), which suggests that the **S1**/PEG8000 film is a promising candidate for constructing a luminescent thermometer. The emission color changes for **S1**/PEG8000 at different temperatures were marked on the Commission Internationale de L'Eclairage (CIE) coordinates. The emission color changed distinctly from yellow with CIE coordinates of (0.47, 0.50) to red (0.55, 0.42) with the variations in the temperature range of 25-60 °C (Figure S9).

The working mechanism of this TLM is based on the regulation of distance between the cationic and anionic components of **S1**. Inside the polymer matrix, the cationic and anionic components

are separated out by the polymer chains. As the temperature increases, the free volume becomes larger and the polymer chain movement becomes more active, creating the scope for the cations and anions to move into proximity with the assistance of electrostatic, Pt···Pt, and π–π stacking interactions (Figure 6g). As a result, the ^{3}MMLCT emission peak at 680 nm was remarkably enhanced, accompanied by the obvious emission color transition from yellow to red. In addition, the appearance of the absorption band at 514 nm also demonstrated the aggregation between the two ions in the ground state (Figures 6a and 6b). When the system cools down to room temperature, two oppositely charged complexes separate out, which gives rise to the recovery of the yellow emission. Also, the thermochromic property of S1/PEG6000 has been investigated. As shown in Figure S10, **S1**/PEG6000 displayed similar emission color change from yellow to orange upon heating. It should be noted that the emission transition temperature of **S1**/PEG6000 is lower than S1/PEG8000. This is because PEG8000 has higher melting point (~62 °C) than that of PEG6000 (~57 °C). These results can further confirm that the thermochromic property is highly associated with the movement of polymer chains upon heating. Notably, the PL spectra remained unchanged upon heating **C1**/PEG8000 and **A1**/PEG8000 films (Figures S5 and S6), which can further demonstrate the key role of electrostatic interactions between the two oppositely charged ions in achieving the thermochromic properties.

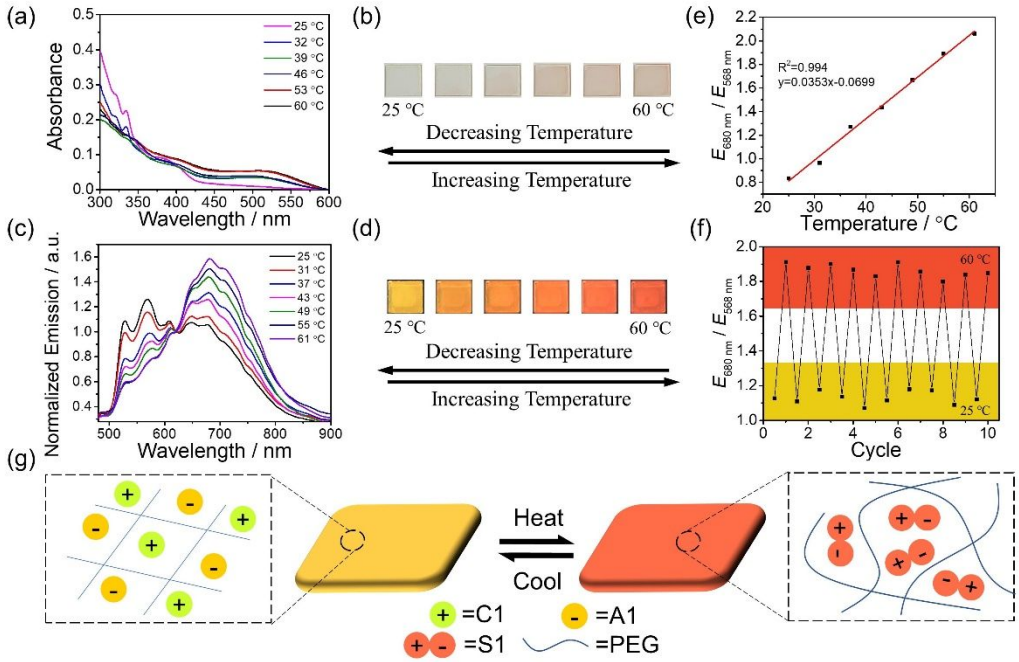

Figure 6. (a) UV−vis absorption spectra of **S1**/PEG8000 (5 wt%) at different temperatures. (b) Photos of **S1**/PEG8000 (5 wt%) upon heating from 25 °C to 60 °C. (c) PL spectra of **S1**/PEG8000 (5 wt%) at different temperatures. (d) Photos of **S1**/PEG8000 (5 wt%) upon heating from 25 °C to 60 °C upon excitation at 365 nm. (e) Temperature dependence of the ratio between E_{680} and E_{568}. (f) 10 cycles of intensity ratio variations measured at 25–60 °C. (g) Schematic illustration describing the thermochromic luminescence induced by reversible intermolecular interactions between two ionic components of **S1**.

Such a remarkable thermochromic performance exhibited by the **S1**/PEG8000 film suggests its strong potential for application in optical anti-counterfeiting. As shown in Figure 7a, the **S1**/PEG8000 film was used as a security ink to produce an anti-counterfeiting label of an apple. The created tag showed distinctly different emission color variation from yellow to red upon heating to 60 °C. When the temperature dropped, the recovery of yellow emission color was observed. Thus, the **S1**/PEG8000 film developed in this work has been demonstrated as a promising candidate for practical applications related to optical anti-counterfeiting.

Furthermore, PLIM technique was employed to achieve higher level anti-counterfeiting applications. A strongly emissive fluorescent dye rhodamine with short emission decay time was used as the background interference to cover the image of number "2" created by the **S1**/PEG8000 film (Figure 7b). Thus, the information was unreadable under a UV excitation. When PLIM was applied, a clear vision of number "2" emerged due to the distinct emission lifetimes of **S1** and rhodamine. More importantly, upon heating to 60 °C, although no detectable variation under UV lamp could be observed, a significant change in the emission lifetime of **S1** produced number "2" under PLIM, its emission lifetime remarkably decreased from 640 ns to 300 ns upon heating (Figures S13 and S14). This can be explained by the intense Pt···Pt interactions between two ions that caused PL property changes, which is in accordance with the results obtained in the solid state. This change is promising in high-level anti-counterfeiting applications, which cannot be encrypted by normal confocal laser scanning microscopy technique.

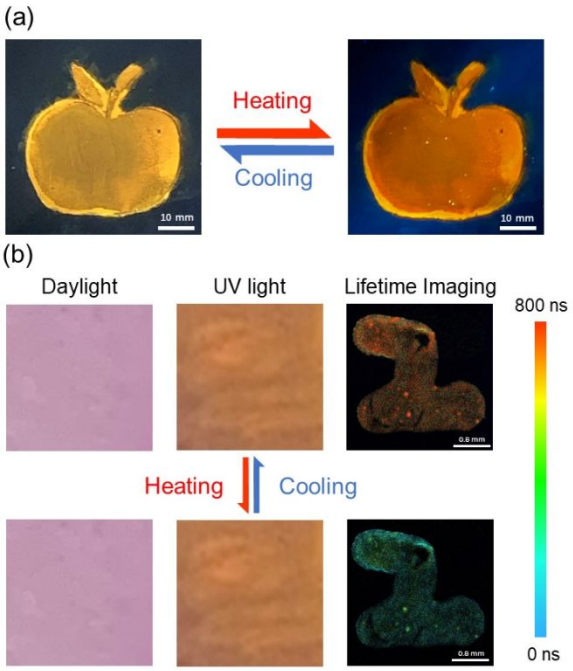

Figure 7. (a) Photographic image of thermochromic luminescent pattern (**S1**/PEG8000, 5 wt%) at different temperatures. (b) Photos of **S1**/PEG8000 pattern with rhodamine as the background fluorescence under daylight, UV excitation, and PLIM.

3. CONCLUSIONS

In summary, a novel soft salt complex **S1** consisting of platinum(II) complexes of opposite charges is reported. The capability of **S1** to assemble into highly ordered nanofibers by the change of DMSO/H_2O composition, accompanied by UV−vis absorption and PL spectral changes is also demonstrated. Such a self-assembly process is governed by the combination of electrostatic, Pt···Pt and π−π stacking interactions between the cationic and anionic platinum(II) complexes. Besides, a thermochromic film was successfully constructed by blending **S1** into PEG8000. The intermolecular interactions between the two oppositely charged complex ions can be altered by changing the temperature owing to the variations in the free volume and polymer chain movement. Consequently, the emission color changed substantially from yellow to red. Finally, by taking advantage of this fantastic thermochromic performance of the **S1**/PEG8000 film, anti-counterfeiting labels have been prepared. Moreover, a high-level anti-counterfeiting application was achieved by using emission lifetime as the analytical signal and PLIM technique. It is anticipated that this design principle based on the manipulation of intermolecular interactions between cationic and anionic platinum(II) complexes can be extended to the development of various stimuli-responsive materials such as electrochromic, mechanochromic, and vapochromic materials.

4. EXPERIMENTAL SECTION

4.1. Materials and Measurements

All starting materials and reagents were acquired commercially and used without further purification. The molecular weight was characterized by quadrupole-orbitrap mass spectrometer (QExactive, ThermoFisher Scientific). ^{1}H NMR (400 MHz) and ^{13}C NMR (100 MHz) spectra were recorded on a Bruker ACF400 spectrometer at 298 K using deuterated solvents. UV-Vis absorption spectra were recorded on a UV-2600 Shi-madzu UV-Vis spectrophotometer. Photoluminescent spectra were measured with an Edinburgh Instrument FLS980 combined with fluorescence lifetime and steady state spectrophotometer that was equipped with a red-sensitive single-photon counting photomultiplier in Peltier Cooled Housing. Fluorescence spectral changes upon heating at different temperatures were recorded on an Ideaoptics Instruments NOVA Fiber optic spectrometer (360–930 nm). Transmission electron microscopy (TEM) experiments were recorded on a Hitachi 7700 Transmission Electron Microscope with an accelerating voltage of 100 kV.

4.2. Synthesis of the dinuclear cyclometalated platinum(II) precursors

The dinuclear cyclometalated platinum(II) precursors $[Pt(C\hat{}N)_2Cl]_2$ were synthesized according to the literature method. K_2PtCl_4 and 2.2 equivalents of HC^N were dissolved in 2-ethoxyethanol (15 mL) and deionized water (5 mL) under an argon flow and heated to 80 ^{o}C for 16 h. After cooling down to room temperature, the mixture was poured into water (30 mL) and the precipitate was washed with deionized water (10 mL × 3). A yellow solid was obtained by vacuum drying.

4.3. Synthesis of C1

The precursors and 3 equivalents of ethylenediamine were added in 20 mL dichloromethane, and the mixture was stirred for 4 h at room temperature under an argon flow. The solvent was removed under reduced pressure, the residue was purified through column chromatography over alumina eluting with dichloromethane and methanol to give the desired product. Yield 82%.^{1}H NMR (400

MHz, DMSO-d_6) δ(ppm): 8.72 (d, J = 4.2 Hz, 1H), 8.21 (m, 2H), 7.94 (d, J = 8.7 Hz, 1H), 7.61 (s, 1H), 7.48 (m, 2H), 6.27 (s, 2H), 5.49 (s, 2H), 2.69 (s, 4H). ^{13}C NMR (100 MHz, DMSO-d_6) δ(ppm): 165.14, 152.01, 149.73, 145.43, 140.72, 130.26, 129.55, 126.19, 125.05, 124.49, 123.48, 120.97, 120.75, 120.71, 48.27, 44.09. Positive ESI-MS: *m/z* = 477.09 (calc. $C_{14}H_{15}F_3N_3Pt$ = 477.09).

4.4. Synthesis of A1

The resulting Pt-dimer was refluxed with 5 equivalents of tetrabutylammonium cyanide at 50 °C for 6 hours with stirring. After cooling down to room temperature, the solvent was removed under reduced pressure. The residue was dissolved in 20 mL dichloromethane and was washed with water (20 mL × 3) to obtain the crude products, and the residue was purified by column chromatography over alumina eluting with dichloromethane and methanol to give the desired product. Yield 67%. ^{1}H NMR (400 MHz, DMSO-d_6) δ(ppm): 9.97 (s, 1H), 9.31 (d, J = 4.1 Hz, 1H), 8.40 (d, J = 1.8 Hz, 1H), 8.22 (d, J = 7.8 Hz, 1H), 8.17 (m, 1H), 7.96 (d, J = 7.9 Hz, 1H), 7.60 (m, 1H), 7.53 (m, 1H), 3.17 (m, 8H), 1.57 (m, 8H), 1.31 (m, 8H), 0.95 (m, 12H). ^{13}C NMR (100 MHz, DMSO-d_6) δ(ppm): 194.26, 165.89, 158.53, 153.05, 143.58, 140.44, 139.38, 136.67, 125.55, 124.32, 121.22, 115.05, 57.99, 23.54, 19.67, 13.96. Negative ESI-MS: *m/z* = 429.03 (calc. $C_{14}H_8N_3OPt$ = 429.03).

4.5. Synthesis of S1

The Pt(II) based soft salt was synthesized through simple metathesis reaction which is modified from the literature. To a 5 mL ethanol solution, 1 equivalent of **A1** and 1.1 equivalents of **C1** were added to obtain a yellow solution. Then the mixed solution was treated under ultrasound for 10 min, the yellow solution became red immediately and red precipitate was formed. Then it was poured into 50 mL deionized water followed by another 30 min of sonication. After removing the solvent by using a centrifuge, the residue was washed with 10 mL deionized water and 10 mL

dichloromethane, and further purified by recrystallization from methanol/ether to acquire the products as a red solid. Yield 76%. ^{1}H NMR (400 MHz, DMSO-d_6) δ(ppm): 9.96 (s, 1H), 9.30 (d, J = 5.9 Hz, 1H), 8.66 (d, J = 5.7 Hz, 1H), 8.40 (s, 1H), 8.19 (m, 4H), 7.94 (t, J = 7.3 Hz, 2H), 7.60 (m, 2H), 7.49 (m, 3H), 6.23 (s, 2H), 5.38 (s, 2H), 2.69 (s, 4H). ^{13}C NMR (100 MHz, DMSO-d_6) δ(ppm): 194.26, 165.86, 165.14, 158.46, 153.16, 153.04, 151.82, 149.70, 145.19, 143.68, 140.78, 140.41, 139.37, 136.66, 130.16, 129.57, 129.27, 126.17, 125.58, 125.54, 125.08, 124.53, 124.31, 123.46, 121.20, 121.02, 120.81, 120.77, 115.20, 48.26, 44.15. Negative ESI-MS: m/z = 429.03 (calc. $C_{14}H_8N_3OPt$ = 429.03)，Positive ESI-MS: m/z = 477.09 (calc. $C_{14}H_{15}F_3N_3Pt$ = 477.09).

4.6. Photoluminescence lifetime imaging

The prepared TLM film was placed on the PLIM setup, which is integrated with Olympus IX81 laser scanning confocal microscope. The photoluminescence signal was detected by the system of the confocal microscope and correlative calculation of the data was carried out by professional software which was provided by Pico Quant Company. The light from the pulse diode laser head (Pico Quant, PDL 800-D) with excitation wavelength of 405 nm and frequency of 0.5 MHz was focused onto the sample with a 40x/NA 0.95 objective lens for single-photon excitation.

4.7. The preparation of the thermochromic luminescent film

5 mg soft salt **S1** was weighed and dissolved in 5.5 mL methanol to prepare a solution with a concentration of 1×10^{-3} M, and 100 mg polyethylene glycol was weighed and dissolved in 1 mL dichloromethane. By calculating the required mass percentage(0.1-5.0 wt%), the corresponding soft salt **S1** solution and polyethylene glycol solution were measured and mixed evenly. For example, 11 μL soft salt **S1** solution and 100 μL polyethylene glycol solution was measured and mixed to prepare 0.1 wt% film. The mixed solution was dripped on the glass substrate (1.5×1.5 cm) by the drop coating method, and the film was prepared after the solvent volatilized.

AUTHOR INFORMATION

Corresponding Author

* E-mail: iamqzhao@njupt.edu.cn (Q. Z.).

* E-mail: wai-yeung.wong@polyu.edu.hk (W.-Y. W).

Notes

The authors declare no competing financial interests.

ACKNOWLEDGMENT

National Funds for Distinguished Young Scientists (61825503) and National Natural Science Foundation of China (51873176, 62075101, 21701087 and 61775101), and Natural Science Foundation of Jiangsu Province of China (BK20200095) were gratefully acknowledged. W.-Y.W. also thanks the financial support from the Hong Kong Research Grants Council (PolyU 153058/19P and C6009-17G), the Hong Kong Polytechnic University (1-ZE1C) and Ms Clarea Au for the Endowed Professorship in Energy (847S).

ASSOCIATED CONTENT

Supporting Information

The Supporting Information is available free of charge.

Additional details of the UV-Vis spectral data, TEM images, SAED results, chromaticity diagram, emission decay curves, ESI-MS data, NMR data.

REFERENCES

(1) (a) Wong, C. L.; Ng, M.; Hong, E. Y.; Wong, Y. C.; Chan, M. Y.; Yam, V. W. Photoresponsive Dithienylethene-Containing Tris(8-hydroxyquinolinato)aluminum(III) Complexes with Photocontrollable Electron-Transporting Properties for Solution-Processable Optical and Organic Resistive Memory Devices. *J. Am. Chem. Soc.* **2020,** *142*, 12193-12206. (b) Gu, Q. F.; He, J. H.; Chen, D. Y.; Dong, H. L.; Li, Y. Y.; Li, H.; Xu, Q. F.; Lu, J. M. Multilevel Conductance Switching of a Memory Device Induced by Enhanced Intermolecular Charge Transfer. *Adv. Mater.* **2015,** *27*, 5968-5973. (c) Leydecker, T.; Herder, M.; Pavlica, E.; Bratina, G.; Hecht, S.; Orgiu, E.; Samori, P. Flexible Non-Volatile Optical Memory Thin-Film Transistor Device with Over 256 Distinct Levels Based on an Organic Bicomponent Blend. *Nat. Nanotechnol.* **2016,** *11*, 769-775.

(2) (a) Zou, H. X.; Hai, Y.; Ye, H. B.; You, L. Dynamic Covalent Switches and Communicating Networks for Tunable Multicolor Luminescent Systems and Vapor-Responsive Materials. *J. Am. Chem. Soc.* **2019,** *141*, 16344-16353. (b) Ma, T. J.; Li, T. T.; Zhou, L. W.; Ma, X. D.; Yin, J.; Jiang, X. S. Dynamic Wrinkling Pattern Exhibiting Tunable Fluorescence for Anticounterfeiting Applications. *Nat. Commun.* **2020,** *11*, 1811.

(3) (a) Chen, L.; Wu, J. C.; Schmuck, C.; Tian, H. A Switchable Peptide Sensor for Real-Time Lysosomal Tracking. *Chem. Commun.* **2014,** *50*, 6443-6446. (b) Heilemann, M.; Dedecker, P.; Hofkens, J.; Sauer, M. Photoswitches: Key Molecules for Subdiffraction-Resolution Fluorescence Imaging and Molecular Quantification. *Laser. Photon. Rev.* **2009,** *3*, 180-202.

(4) (a) Mao, Z.; Yang, Z.; Mu, Y.; Zhang, Y.; Wang, Y. F.; Chi, Z.; Lo, C. C.; Liu, S.; Lien, A.; Xu, J. Linearly Tunable Emission Colors Obtained from a Fluorescent-Phosphorescent Dual-Emission Compound by Mechanical Stimuli. *Angew. Chem. Int. Ed.* **2015,** *54*, 6270-6273. (b) Ma, Y.; Yu, Y. X.; She, P. F.; Lu, J. Y.; Liu, S. J.; Huang, W.; Zhao, Q. On-Demand Regulation of

Photochromic Behavior Through Various Counterions for High-Level Security Printing. *Sci. Adv.* **2020,** *6*, Eaaz2386.

(5) (a) Ma, Y.; Dong, Y. F.; Liu, S. Y.; She, P. F.; Lu, J. Y.; Liu, S. J.; Huang, W.; Zhao, Q. Chameleon-Like Thermochromic Luminescent Materials with Controllable Response Behaviors for Multilevel Security Printing. *Adv. Opt. Mater.* **2020,** *8*, 1901687. (b) Jiang, K.; Wang, Y. H.; Cai, C. Z.; Lin, H. W. Conversion of Carbon Dots from Fluorescence to Ultralong Room-Temperature Phosphorescence by Heating for Security Applications. *Adv. Mater.* **2018,** *30*, 1800783.

(6) (a) Wei, P. F.; Zhang, J.-X.; Zhao, Z.; Chen, Y. C.; He, X. W.; Chen, M.; Gong, J. Y.; Sung, H. H.-Y.; Williams, I. D.; Lam, J. W. Y. Multiple Yet Controllable Photoswitching in a Single Aiegen System. *J. Am. Chem. Soc.* **2018,** *140*, 1966-1975. (b) Mutoh, K.; Miyashita, N.; Arai, K.; Abe, J. Turn-on Mode Fluorescence Switch by Using Negative Photochromic Imidazole Dimer. *J. Am. Chem. Soc.* **2019,** *141*, 5650-5654. (c) Kometani, A.; Inagaki, Y.; Mutoh, K.; Abe, J. Red or Near-Infrared Light Operating Negative Photochromism of a Binaphthyl-Bridged Imidazole Dimer. *J. Am. Chem. Soc.* **2020,** *142*, 7995-8005.

(7) (a) Zhang, W. R.; Zhang, Y. M.; Xie, F. L.; Jin, X. C.; Li, J.; Yang, G. J.; Gu, C.; Wang, Y. Y.; Zhang, S. X. A. A Single-Pixel RGB Device in a Colorful Alphanumeric Electrofluorochromic Display. *Adv. Mater.* **2020**, 2003121. (b) Wang, Y. Y.; Wang, S.; Wang, X. J.; Zhang, W. R.; Zheng, W. X.; Zhang, Y.-M.; Zhang, S. X.-A. A Multicolour Bistable Electronic Shelf Label Based on Intramolecular Proton-Coupled Electron Transfer. *Nat. Mater.* **2019,** *18*, 1335-1342.

(8) (a) Zhao, W. J.; He, Z. K.; Peng, Q.; Lam, J. W. Y.; Ma, H. L.; Qiu, Z. J.; Chen, Y. C.; Zhao, Z.; Shuai, Z. G.; Dong, Y. Q. Highly Sensitive Switching of Solid-State Luminescence by Controlling Intersystem Crossing. *Nat. Commun.* **2018,** *9*, 3044. (b) He, Z. H.; Gao, H. Q.; Zhang,

S. T.; Zheng, S. Y.; Wang, Y. Z.; Zhao, Z. H.; Ding, D.; Yang, B.; Zhang, Y. M.; Yuan, W. Z. Achieving Persistent, Efficient, and Robust Room-Temperature Phosphorescence from Pure Organics for Versatile Applications. *Adv. Mater.* **2019,** *31*, 1807222. (c) Hupp, B.; Nitsch, J.; Schmitt, T.; Bertermann, R.; Edkins, K.; Hirsch, F.; Fischer, I.; Auth, M.; Sperlich, A.; Steffen, A. Stimulus-Triggered Formation of an Anion-Cation Exciplex in Copper (I) Complexes as a Mechanism for Mechanochromic Phosphorescence. *Angew. Chem. Int. Ed.* **2018,** *57*, 13671-13675.

(9) (a) Kar, P.; Yoshida, M.; Shigeta, Y.; Usui, A.; Kobayashi, A.; Minamidate, T.; Matsunaga, N.; Kato, M. Methanol-Triggered Vapochromism Coupled with Solid-State Spin Switching in a Nickel (II)-Quinonoid Complex. *Angew. Chem. Int. Ed.* **2017,** *129*, 2385-2389. (b) Lien, C.-Y.; Hsu, Y.-F.; Liu, Y.-H.; Peng, S.-M.; Shinmyozu, T.; Yang, J.-S. Steric Engineering of Cyclometalated Pt (II) Complexes Toward High-Contrast Monomer–Excimer-Based Mechanochromic and Vapochromic Luminescence. *Inorg. Chem.* **2020,** *59*, 11584-11594. (c) Luong, L. M.; Malwitz, M. A.; Moshayedi, V.; Olmstead, M. M.; Balch, A. L. Role of Anions and Mixtures of Anions on The Thermochromism, Vapochromism, and Polymorph Formation of Luminescent Crystals of a Single Cation, $[(C_6H_{11}NC)_2Au]^+$. *J. Am. Chem. Soc.* **2020,** *142*, 5689-5701.

(10) (a) Pan, Y.; Xie, X.-J.; Huang, Q.-W.; Gao, C.; Wang, Y.-B.; Wang, L.-X.; Yang, B.-X.; Su, H. Q.; Huang, L.; Huang, W. Inherently Eu_2^+/Eu_3^+ Codoped Sc_2O_3 Nanoparticles as High-Performance Nanothermometers. *Adv. Mater.* **2018,** *30*, 1705256. (b) Jing, C.-Q.; Wu, J.-H.; Cao, Y.-Y.; Che, H.-X.; Zhao, X.-M.; Yue, M.; Liao, Y.-Y.; Yue, C.-Y.; Lei, X.-W. A Three-Dimensional Cuprous Lead Bromide Framework with Highly Efficient and Stable Thermochromic Luminescence Properties. *Chem. Commun.* **2020,** *56*, 5925-5928. (c) Du, J. H.; Sheng, L.; Chen,

Q.-N.; Xu, Y.; Li, W.; Wang, X.-J.; Li, M.-J.; Zhang, S. X.-A. Simple and General Platform for Highly Adjustable Thermochromic Fluorescent Materials and Multi-Feasible Applications. *Mater. Horizon.* **2019,** *6*, 1654-1662.

(11) (a) Guo, Y. X.; Gu, S. Z.; Feng, X.; Wang, J. N.; Li, H. W.; Han, T. Y.; Dong, Y. P.; Jiang, X.; James, T. D.; Wang, B. 3D Cross-Correlative Matrix Temperature Detection and Non-Invasive Thermal Mapping Based on a Molecular Probe. *Chem. Sci.* **2014,** *5*, 4388-4393. (b) Zhang, Y. Y.; Li, Y. R.; Wang, H.; Zhang, Z. Y.; Feng, Y. L.; Tian, Q.; Li, N.; Mei, J.; Su, J. H.; Tian, H. Measuring The Microphase Separation Scale of Polyurethanes with a Vibration-Induced Emission-Based Ratiometric "Fluorescent Ruler". *ACS. Appl. Mater. Interfaces.* **2019,** *11*, 39351-39358. (c) Irie, M.; Fukaminato, T.; Matsuda, K.; Kobatake, S. Photochromism of Diarylethene Molecules and Crystals: Memories, Switches, and Actuators. *Chem. Rev.* **2014,** *114*, 12174-12277.

(12) (a) Ma, Y.; Shen, L.; She, P. F.; Hou, Y. Q.; Yu, Y. X.; Zhao, J. Z.; Liu, S. J.; Zhao, Q. Constructing Multi-Stimuli-Responsive Luminescent Materials Through Outer Sphere Electron Transfer in Ion Pairs. *Adv. Opt. Mater.* **2019,** *7*, 1801657. (b) Shigeta, Y.; Kobayashi, A.; Yoshida, M.; Kato, M. Stability Tuning of Vapor-Adsorbed State of Vapochromic Pt (II) Complex by Introduction of Chiral Moiety. *Inorg. Chem.* **2019,** *58*, 7385-7392. (c) Zhao, K.-Y.; Mao, H.-T.; Wen, L.-L.; Shan, G.-G.; Fu, Q.; Sun, H.-Z.; Su, Z.-M. A Simple Strategy to Achieve Remarkable Mechanochromism of Cationic Ir(III) Phosphors Through Subtle Ligand Modification. *J. Mater. Chem. C.* **2018,** *6*, 11686-11693.

(13) (a) Ding, Y. Y.; Jiang, S. L.; Gao, Y. J.; Nie, J.; Du, H. G.; Sun, F. Photochromic Polymers Based on Fluorophenyl Oxime Ester Photoinitiators as Photoswitchable Molecules. *Macromolecules.* **2020,** *53*, 5701-5710. (b) Calvino, C.; Guha, A.; Weder, C.; Schrettl, S. Self-

Calibrating Mechanochromic Fluorescent Polymers Based on Encapsulated Excimer-Forming Dyes. *Adv. Mater.* **2018,** *30*, 1704603.

(14) (a) Kundu, P. K.; Samanta, D.; Leizrowice, R.; Margulis, B.; Zhao, H.; Börner, M.; Udayabhaskararao, T.; Manna, D.; Klajn, R. Light-Controlled Self-Assembly of Non-Photoresponsive Nanoparticles. *Nat. Chem.* **2015,** *7*, 646-652. (b) Wang, W. S.; Feng, J.; Ye, Y. F.; Lyu, F. L.; Liu, Y.-S.; Guo, J. H.; Yin, Y. D. Photocatalytic Color Switching of Transition Metal Hexacyanometalate Nanoparticles for High-Performance Light-Printable Rewritable Paper. *Nano. Lett.* **2017,** *17*, 755-761.

(15) (a) You, Y.; Nam, W. Photofunctional Triplet Excited States of Cyclometalated Ir(III) Complexes: Beyond Electroluminescence. *Chem. Soc. Rev.* **2012,** *41*, 7061-7084. (b) Sasabe, H.; Takamatsu, J. I.; Motoyama, T.; Watanabe, S.; Wagenblast, G.; Langer, N.; Molt, O.; Fuchs, E.; Lennartz, C.; Kido, J. High-Efficiency Blue and White Organic Light-Emitting Devices Incorporating a Blue Iridium Carbene Complex. *Adv. Mater.* **2010,** *22*, 5003-5007. (c) Chen, Z. Q.; Bian, Z. Q.; Huang, C. H. Functional IrIII Complexes and Their Applications. *Adv. Mater.* **2010,** *22*, 1534-1539.

(16) (a) Martir, D. R.; Zysman-Colman, E. Supramolecular Iridium(III) Assemblies. *Coord. Chem. Rev.* **2018,** *364*, 86-117. (b) Ma, Y.; Chen, K. X.; Guo, Z. L.; Liu, S. J.; Zhao, Q.; Wong, W.-Y. Phosphorescent Soft Salt Complexes for Optoelectronic Applications. *Acta. Chim. Sinica.* **2020,** *78*, 23-33.

(17) (a) Wu, C.; Chen, H.-F.; Wong, K.-T.; Thompson, M. E. Study of Ion-Paired Iridium Complexes (Soft Salts) and Their Application in Organic Light Emitting Diodes. *J. Am. Chem. Soc.* **2010,** *132*, 3133-3139. (b) Nasr, G.; Guerlin, A.; Dumur, F.; Beouch, L.; Dumas, E.; Clavier, G.; Miomandre, F.; Goubard, F.; Gigmes, D.; Bertin, D. Iridium (III) Soft Salts from Dinuclear

Cationic and Mononuclear Anionic Complexes for OLED Devices. *Chem. Commun.* **2011,** *47*, 10698-10700. (c) Dumur, F.; Nasr, G.; Wantz, G.; Mayer, C. R.; Dumas, E.; Guerlin, A.; Miomandre, F.; Clavier, G.; Bertin, D.; Gigmes, D. Cationic Iridium Complex for The Design of Soft Salt-Based Phosphorescent Oleds and Color-Tunable Light-Emitting Electrochemical Cells. *Org. Electron.* **2011,** *12*, 1683-1694.

(18) Ma, Y.; Liang, H.; Zeng, Y.; Yang, H. R.; Ho, C.-L.; Xu, W. J.; Zhao, Q.; Huang, W.; Wong, W.-Y. Phosphorescent Soft Salt for Ratiometric and Lifetime Imaging of Intracellular Ph Variations. *Chem. Sci.* **2016,** *7*, 3338-3346.

(19) Ma, Y.; Zhang, S. J.; Wei, H. J.; Dong, Y. F.; Shen, L.; Liu, S. J.; Zhao, Q.; Liu, L.; Wong, W.-Y. Enhanced Singlet Oxygen Generation of a Soft Salt Through Efficient Energy Transfer Between Two Ionic Metal Complexes. *Dalton. Trans.* **2018,** *47*, 5582-5588.

(20) (a) Liu, Q.; Xie, M.; Chang, X. Y.; Cao, S.; Zou, C.; Fu, W. F.; Che, C. M.; Chen, Y.; Lu, W. Tunable Multicolor Phosphorescence of Crystalline Polymeric Complex Salts with Metallophilic Backbones. *Angew. Chem. Int. Ed.* **2018,** *57*, 6279-6283. (b) Mauro, M.; Schuermann, K. C.; PrÉTôt, R.; Hafner, A.; Mercandelli, P.; Sironi, A.; De Cola, L. Complex Iridium (III) Salts: Luminescent Porous Crystalline Materials. *Angew. Chem. Int. Ed.* **2010,** *49*, 1222-1226.

(21) (a) Wong, W.-Y.; Ho, C.-L. Functional Metallophosphors for Effective Charge Carrier Injection/Transport: New Robust OLED Materials with Emerging Applications. *J. Mater. Chem.* **2009,** *19*, 4457-4482. (b) Chou, P. T.; Chi, Y. Phosphorescent Dyes for Organic Light-Emitting Diodes. *Chem. Eur. J.* **2007,** *13*, 380-395.

(22) (a) She, P. F.; Ma, Y.; Qin, Y. Y.; Xie, M. J.; Li, F. Y.; Liu, S. J.; Huang, W.; Zhao, Q. Dynamic Luminescence Manipulation for Rewritable and Multi-Level Security Printing. *Matter.* **2019,** *1*, 1644-1655. (b) Lu, Y. Q.; Zhao, J. B.; Zhang, R.; Liu, Y. J.; Liu, D. M.; Goldys, E. M.;

Yang, X. S.; Xi, P.; Sunna, A.; Lu, J. Tunable Lifetime Multiplexing Using Luminescent Nanocrystals. *Nat. Photonics.* **2014,** *8*, 32-36. (c) Dong, H.; Sun, L.-D.; Feng, W.; Gu, Y. Y.; Li, F. Y.; Yan, C.-H. Versatile Spectral and Lifetime Multiplexing Nanoplatform with Excitation Orthogonalized Upconversion Luminescence. *ACS. Nano.* **2017,** *11*, 3289-3297.

(23) (a) Wong, V. C.-H.; Po, C.; Leung, S. Y.-L.; Chan, A. K.-W.; Yang, S. Y.; Zhu, B. R.; Cui, X. D.; Yam, V. W.-W. Formation of 1D Infinite Chains Directed by Metal-Metal and/or π–π Stacking Interactions of Water-Soluble Platinum (II) 2, 6-Bis (Benzimidazol-2′-yl) Pyridine Double Complex Salts. *J. Am. Chem. Soc.* **2018,** *140*, 657-666. (b) Au-Yeung, H.-L.; Tam, A. Y.-Y.; Leung, S. Y.-L.; Yam, V. W.-W. Supramolecular Assembly of Platinum-Containing Polyhedral Oligomeric Silsesquioxanes: An Interplay of Intermolecular Interactions and a Correlation Between Structural Modifications and Morphological Transformations. *Chem. Sci.* **2017,** *8*, 2267-2276. (c) Chan, M. H.-Y.; Leung, S. Y.-L.; Yam, V. W.-W. Rational Design of Multi-Stimuli-Responsive Scaffolds: Synthesis of Luminescent Oligo (Ethynylpyridine)-Containing Alkynylplatinum (II) Polypyridine Foldamers Stabilized by Pt···Pt Interactions. *J. Am. Chem. Soc.* **2019,** *141*, 12312-12321. (d) Aliprandi, A.; Genovese, D.; Mauro, M.; De Cola, L. Recent Advances in Phosphorescent Pt(II) Complexes Featuring Metallophilic Interactions: Properties and Applications. *Chem. Lett.* **2015,** *44*, 1152-1169. (e) Ly, K. T.; Chen-Cheng, R.-W.; Lin, H.-W.; Shiau, Y.-J.; Liu, S.-H.; Chou, P.-T.; Tsao, C.-S.; Huang, Y.-C.; Chi, Y. Near-Infrared Organic Light-Emitting Diodes with Very High External Quantum Efficiency and Radiance. *Nat. Photonics.* **2017,** *11*, 63-68.

(24) Rausch, A. F.; Monkowius, U.V.; Zabel, M.; Yersin, H. Bright Sky-Blue Phosphorescence of [n-Bu_4N][Pt(4,6-dFppy)$(CN)_2$]: Synthesis, Crystal Structure, and Detailed Photophysical Studies. *Inorg. Chem.* **2010**, *49*, 7818–7825.

(25) Yersin, H.; Donges, D. Low-Lying Electronic States and Photophysical Properties of Organometallic Pd(II) and Pt(II) Compounds. Modern Research Trends Presented in Detailed Case Studies. *Top. Curr. Chem.* **2001**, *214*, 81

(26) Li, Y. G.; Chen, L.; Ai Y. Y.; Hong, E. Y-H.; Chan, A. K-W.; Yam, V. W-W. Supramolecular Self-Assembly and Dual-Switch Vapochromic, Vapoluminescent, and Resistive Memory Behaviors of Amphiphilic Platinum(II) Complexes. *J. Am. Chem. Soc.* **2017**, *139*, 13858–13866

(27) Po, C.; Tam, A. Y-Y.; Wong, K. M-C.; Yam, V. W-W. Supramolecular Self-Assembly of Amphiphilic Anionic Platinum(II) Complexes: A Correlation between Spectroscopic and Morphological Properties. *J. Am. Chem. Soc.* **2011**, *133*, 12136–12143

(28) Liu, X.; Li, S. Y.; Feng, J.; Li, Y.; Yang, G. Q. A Triarylboron-Based Fluorescent Temperature Indicator: Sensitive Both in Solid Polymers and in Liquid Solvents. *Chem. Commun*. **2014,** *50*. 2778-2780.

(29) Brites, C. D. S.; Millan, A.; Carlos, L. D. Lanthanides in Luminescent Thermometry, *Handbook on the Physics and Chemistry of Rare Earths*, Elsevier Science B. V., Amsterdam, **2016**, Ch. 281, vol. 49, pp. 339–427.